Noruzi *et al. Chem. Biol. Technol. Agric.* (2023) 10:71
https://doi.org/10.1186/s40538-023-00437-0

Chemical and Biological Technologies in Agriculture

RESEARCH

Open Access

Hydroxyapatite nanoparticles: an alternative to conventional phosphorus fertilizers in acidic culture media

Masumeh Noruzi[1*], Parvin Hadian[1], Leila Soleimanpour[2], Leila Ma'mani[1] and Karim Shahbazi[3]

Abstract

Background Traditional phosphorus fertilizers generally have low efficiencies due to their immobilization in soil, and a large part of these fertilizers are not plant-available. Also, phosphorus resources are non-renewable. In recent years, a great deal of attention has been paid to nanofertilizers because of their slow or controlled release and also their very small particle size which increases the solubility and uptake of nanoparticles in plant. Hydroxyapatite nanoparticles are of great importance as phosphorus nanofertilizer thanks to their very low toxicity, biocompatibility, and the fact that products obtained from their degradation, i.e., phosphate and calcium ions, are naturally available in soils.

Results In this study, hydroxyapatite nanoparticles were synthesized using the wet chemical precipitation method in three formulations and characterized with various techniques including electron microscopy, atomic force microscopy, X-ray diffraction, Fourier-transform infrared spectroscopy, and elemental analysis. Chemical and microscopic analyses showed that phosphorus was distributed in different parts of the wheat (*Triticum aestivum* L.) plant. To investigate the fertilizing effects of the nanoparticles, hydroxyapatite nanoparticles were used in different culture media including alkaline soil, acidic soil, the mixture of peat moss and perlite, and cocopeat. Based on our observations, hydroxyapatite nanoparticles showed fertilizing properties in all media. However, fertilizing potential strongly depended on the culture media. HAP nanoparticles demonstrated a high potential to be used as a fertilizer in acidic media. Nevertheless, only a slight fertilizing effect was observed in alkaline soils. Furthermore, the findings of our study showed fertilizing properties of powder hydroxyapatite nanoparticles without the need to convert them to suspension. Moreover, hydroxyapatite nanoparticles in all the three formulations showed low toxicity in such a way that their toxicity was even less than that of triple super phosphate.

Conclusions Hydroxyapatite nanoparticles in both suspension and powder forms can be considered an alternative to conventional phosphorus fertilizers in acidic culture media. Our study revealed that hydroxyapatite nanoparticles were likely dissolved in the culture media and absorbed by plant mainly in the phosphate form.

Keywords Fertilizer, Hydroxyapatite nanoparticles, Phosphorus, Wheat

*Correspondence:
Masumeh Noruzi
mnoruzi@abrii.ac.ir; masumehnoruzi@gmail.com
Full list of author information is available at the end of the article

Graphical Abstract

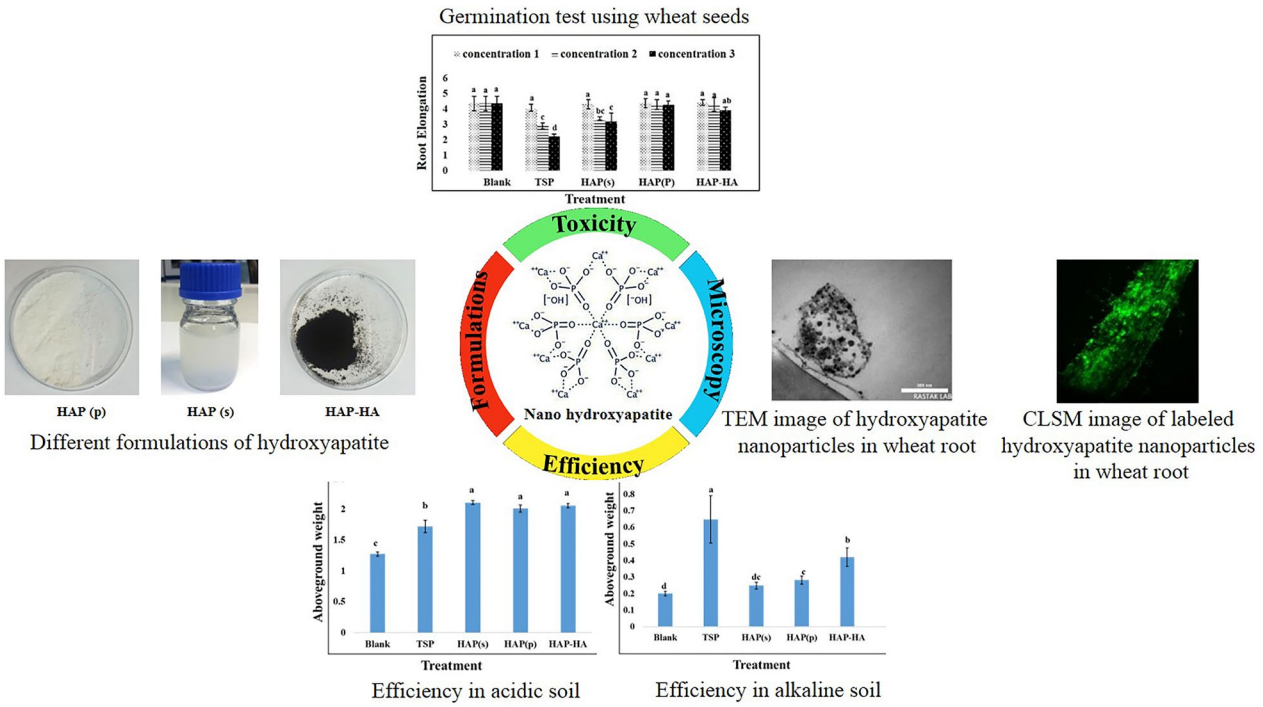

Introduction

The increase in the world's population and the growing of global demand for food have underlined the need for fertilizer supplies in agriculture [1]. Phosphorus (P) is the second essential macronutrient for plant growth after nitrogen (N) [2]. However, the use of traditional P fertilizers has caused some serious problems. P is fixed in soil due to its reaction with Al/Fe and calcium compounds. Thus, its availability for plants significantly decreases [3] in a way that it is estimated that 5.7 billion ha of agricultural land face a lack of plant-available P [4]. In addition, P has a non-renewable nature [1]. In other words, P resources in the world like rock phosphates that are used in the production of conventional fertilizers are limited [5, 6]. Moreover, the high water solubility of P fertilizers and their over-application which is due to their low efficiency have caused eutrophication and environmental contaminations [1, 7]. As a result, researchers are looking for new formulations for P fertilizers to address the above-mentioned problems. With the introduction of nanotechnology in agriculture, P-based nanofertilizers have been considered to be alternatives to conventional P fertilizers. The slow-release characteristic of nanofertilizers can remarkably improve their efficiencies compared to conventional fertilizers [8, 9]. Furthermore, very low solubility of these nanofertilizers minimizes environmental problems such as eutrophication [7]. In recent years, researchers have focused on the use of hydroxyapatite (HAP) nanoparticles as a P nanofertilizer thanks to their biocompatibility, low toxicity, and the fact that the products obtained from their degradation, i.e., phosphate and calcium ions, are naturally available in soil [3, 10]. HAP ($Ca_{10}PO_4(_6)(OH)_2$) is a naturally occurring material and the main component of teeth and bones structure in the human body [5]. One of the first studies on fertilizing properties of HAP nanoparticles was done by Liu et al. [7]. They evaluated the effect of HAP nanoparticles on *Glycine max* growth in a mixture of peat moss and perlite. The study revealed that HAP nanoparticles had fertilizing properties and that their efficiency was significantly higher than that of triple super phosphate (TSP) as a conventional P fertilizer. In the study conducted by Montalvo et al., the effect of HAP nanoparticles on wheat growth was investigated in acidic soils [5]. It was found that fertilizing properties of HAP nanoparticles were significantly higher than bulk HAP. However, nanoparticles showed lower efficiency compared to TSP. The results of Montalvo et al.'s study were in contrast with those of another study [8] where Xiong et al. reported higher efficiency of HAP nanoparticles in comparison

with traditional P fertilizers in acidic soils. In a study conducted in 2018, the investigation of the efficacy of citric acid-modified HAP nanoparticles on *Zea mays* showed that these nanoparticles had a fertilizing potential higher than conventional P fertilizers [1]. The use of HAP nanoparticles as foliar application on rosemary (*Rosmarinus officinalis* L.) demonstrated an increase in growth factors and essential oils production in comparison with traditional fertilizers [11]. Some studies have also reported the use of HAP nanoparticles as carriers for the preparation of slow-release N fertilizers [12, 13]. Nevertheless, the studies on the fertilizing potential of HAP nanoparticles are limited, and most of them have been done in only one type of culture medium. In addition, according to the literature, HAP nanoparticles have been generally applied only in suspension form, i.e., either they have been synthesized in the form of suspension or synthesized powder nanoparticles have been converted to suspension using sonication before applying to the plant. In the present study, HAP nanoparticles were prepared in three formulations, including HAP(s) (i.e., HAP in suspension form), HAP(p) (i.e., HAP in powder form), and HAP-HA (humic acid-modified HAP) using wet chemical precipitation, and their fertilizing effects on wheat growth were investigated in different culture media, including alkaline soil, acidic soil, the mixture of peat moss and perlite, and cocopeat through greenhouse studies. Moreover, uptake of nanoparticles in different parts of the plant as well as the toxicity of HAP nanoparticles were studied.

Experimental

Materials

Calcium hydroxide and carboxy methylcellulose sodium salt (CMC) that were used in HAP synthesis were purchased from Merck and Sigma, respectively. Alizarin red S (ARS) and fluorescein isothiocyanate (FITC) dyes were also obtained from Merck and Sigma, respectively. Humic acid (HA) (as potassium (K) salt) was prepared from Quimical Tierra. 3-Aminopropyltriethoxy silane (APTES) and all the acids used in this study were purchased from Sigma. The chemicals used in preparation of the plant for transmission electron microscopy (TEM) analysis were obtained as follows: glutaraldehyde, osmium tetroxide, and Reynolds solution were obtained from TAAB laboratories-3 Minerva. Uranyl acetate was purchased from BDH Laboratory Chemicals Division. Also, methanol and PBS were obtained from Sigma. Reagents of P analysis, i.e., potassium dihydrogen phosphate, ammonium molybdate, and potassium antimony tartrate, were purchased from Sigma. Also, ascorbic acid and ammonium vanadate were purchased from Duchefa and Riedel-de Haen, respectively. Urea and potassium sulphate were obtained from Sigma and were used as N and K fertilizers.

Preparation of HAP(p) and HAP(s) nanoparticles

HAP(p) (Fig. 1, a-left) and HAP(s) (Fig. 1, a-middle) nanoparticles were synthesized according to the previous reports with few modifications [7, 14]. To synthesize HAP(p) nanoparticles, 0.2 g of calcium hydroxide was added to distilled water and was stirred. Then, 3.2 mL of 0.5 M phosphoric acid was added drop-wise to calcium hydroxide slurry and vigorously stirred for 1 h at room temperature (Ca/P molar ratio should be equal to 1.67). The nanoparticles were collected by centrifuge, washed with distilled water, and dried in a vacuum oven at 60 °C [14]. To prepare HAP(s) nanoparticles, 50 mL of 1% CMC solution was added drop-wise to 0.2 g of calcium hydroxide slurry and stirred overnight at room temperature. Then, 3.2 mL of phosphoric acid solution (0.5 M) was added drop-wise to the mixture while the reaction mixture was vigorously stirred [7]. The reaction lasted for 1 h. The suspension was stable for several months without any visible sediment.

Characterization of nanoparticles

The solubility of nanoparticles in water and the P amounts in fertilizers were measured by Lambda 35 UV–Vis spectroscopy (Perkin Elmer). X-ray diffraction (XRD) experiments were performed by Philips X'pert MPD system with Co Kα radiation (λ: 1.78897 Å) in the 2θ range of 10–80 operated at a voltage of 40 kV and a current of 40 mA. TEM images were obtained using the EM208S Philips instrument at an accelerating voltage of 100 kV. Before imaging, the sample was sonicated using an ultrasonic bath for 15 min. Next, a drop of the sample was placed on a copper grid and after drying it was imaged. CHN elemental analyses were conducted using a Costech ECS 4010 elemental combustion system. 5 mg of the samples were weighed and placed in tin capsules. Furnace temperature was 1050 °C. A 2 m × 5 mm I.D. HayeSep Q 60/80 GC column was used for separating the gases. A thermal conductivity detector was used to determine the amounts of the gases. Helium was used as the carrier gas at a flow rate of 100 mL/min. The P amounts in the plant were measured using inductively coupled plasma-atomic emission spectroscopy (ICP-AES) by the Varian Vista Pro instrument. Atomic emission was measured at 213.618 nm. The external calibration curve method was used in the concentration range of 0.1–20 ppm in the quantitative analysis of P. Instrumental operating conditions were as follows: plasma gas flow rate (argon) and the sample aspiration rate were 1 L/min and 2.5 mL/min, respectively. RF generator frequency was 40 MHz and

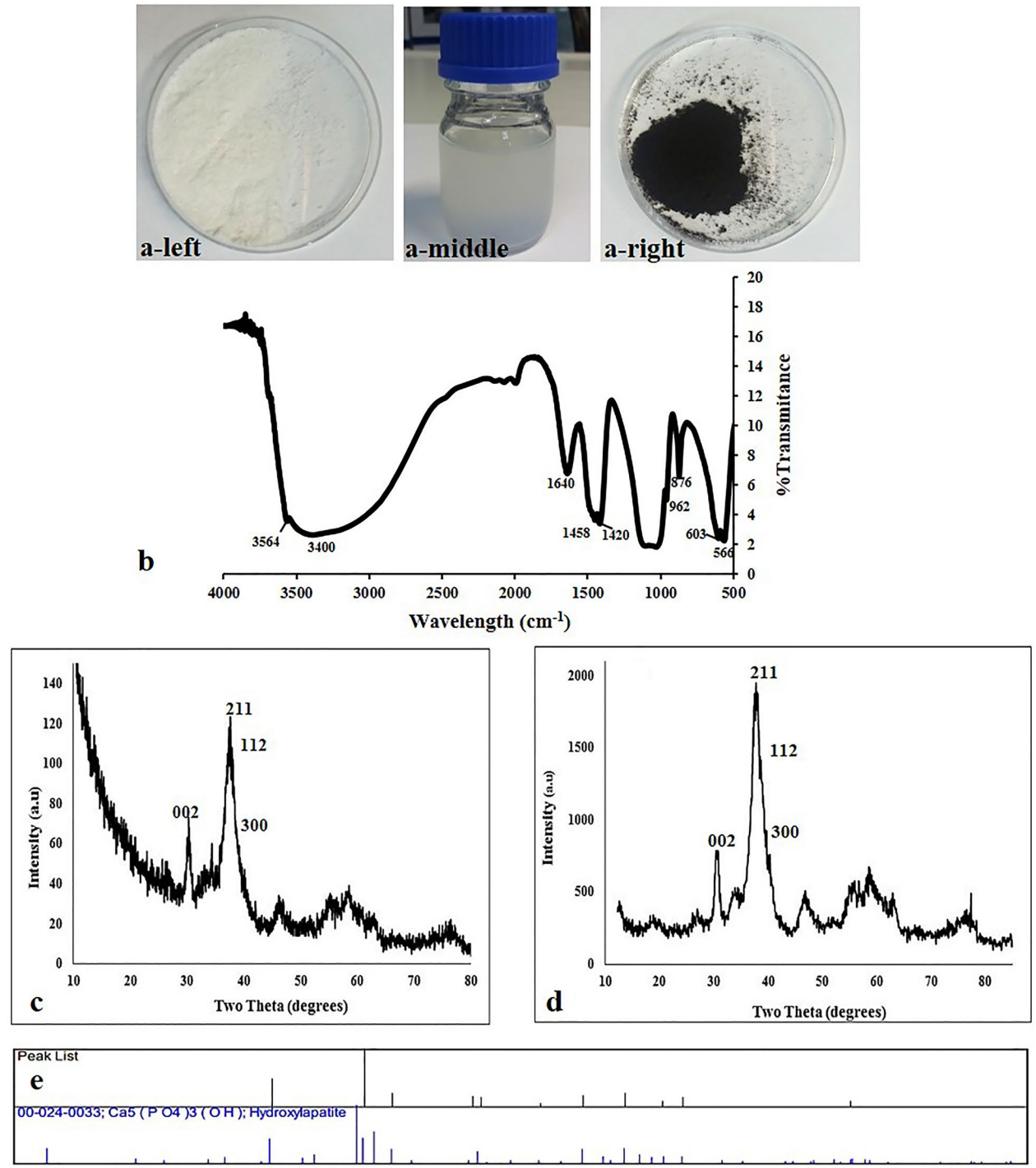

Fig. 1 The images of different formulations of HAP nanoparticles (**a**): HAP(p) (a-left), HAP(s) (a-middle), and HAP-HA(a-right). FT-IR spectrum of HAP(p) nanoparticles (**b**), XRD pattern of HAP(p) nanoparticles (**c**), and XRD pattern of HAP(s) nanoparticles (**d**), standard XRD pattern of HAP (JCPDS Card No. 24-0033) (**e**). Abbreviations: HAP(p), hydroxyapatite nanoparticles in powder form; HAP(s), hydroxyapatite nanoparticles in suspension form; HAP-HA, humic acid-modified hydroxyapatite nanoparticles

it was adjusted to a power of 1150 W. Scanning electron microscopy (SEM) images were taken using a TESCAN SEM. First, conductive carbon tape was mounted on an aluminum stub. Then, very little amounts of the sample were placed on it and the sample was placed in the physical vapor deposition instrument (20% power)

for gold sputtering. Gold coating lasted 140 s. Next, the sample was placed in SEM stage and imaged at an accelerating voltage of 15 kV. Fourier transform infrared (FT-IR) spectra of the samples were obtained by Jasco FT-IR 410 in transmission mode using the KBr pellet technique. A small amount of the sample was blended with spectroscopic grade KBr in an agar mortar and was pressed into a KBr pellet using a hydraulic press under a pressure of 10 tones/cm^2 for 5 min. Then, the sample was placed in the path of infrared beam and the spectra were obtained as an average of 50 measurements in the wavelength range of 500–4000 cm^{-1} at a resolution of 2 cm^{-1}. Confocal laser scanning microscopy (CLSM) analyses were performed by Nikon PCM-2000 equipped with He/Ne (543 nm) and Ar (488 nm) lasers and coupled to an Eclipse E-800 upright microscope. The hand-cut roots and shoots were placed on glass slides and imaging experiments were performed at excitation/emission wavelengths of 495/518 nm and 546/590 nm for FITC and ARS, respectively. Atomic force microscopy (AFM) imaging was performed by a DME SPM microscope equipped with a DS95-50E scanner. Before imaging, the sample was sonicated in a water bath using distilled water as a dispersant. Next, a drop of the sample was placed on mica and after drying was imaged. In AFM analysis, the non-contact working mode was used with an AC probe and the radius of tip curvature was less than 10 nm. The AFM instrument was equipped with alumina-coated silicon cantilever. The force constant of the cantilever was 42 N/m, and the length, width, and thickness of cantilever were 160, 45, and 4.6 μm, respectively. All the experiments were conducted under air atmosphere.

Plant preparation for TEM analysis

To detect nanoparticles in plant using TEM, the wheat seedlings treated with HAP(s) nanoparticles were removed from the soil 1 month after planting and the roots were washed with distilled water several times. To prepare the plant for TEM analysis, wheat roots were cut in 5 mm sections and prefixed in 2.5% glutaraldehyde in PBS (pH: 7.2) for 2 h at 4 °C. Next, these sections were washed with PBS buffer. After being washed, the plant samples were post-fixed in osmium tetroxide (0.5%) in the same buffer at room temperature for 1 h. Then, the samples were dehydrated in an ascending alcohol series and were finally embedded in resin. 50-nm ultra-thin sections were then prepared using ultratome, placed on 300 mesh copper grid and double-stained with 20% uranyl acetate in pure methanol and Reynolds solution for 45 min [15]. Finally, the images of the samples were taken using TEM.

Table 1 Physico-chemical characteristics of the soils

Soil type	Soil pH	N (%)	P (ppm)	K (ppm)	C (%)
Acidic soil	5	0.21	2.4	153	0.98
Alkaline soil	7.6	0.11	3.6	68	0.37

Table 2 The amounts of P in HAP formulations and TSP

Fertilizers	P concentration
HAP(s)	650 ppm
HAP(p)	17.1%
HAP-HA	13.2%
TSP	19.8%

Soil properties and culture media

To investigate the fertilizing properties of HAP nanoparticles, wheat was selected as a model plant. In this study, different growth media, i.e., a mixture of peat moss and perlite (50:50 v/v), cocopeat, acidic soil, and alkaline soil, were investigated. Acidic soil was a sandy loam soil (sand 54%, silt 25%, and clay 21%) and was brought from Gilan province in Iran. Alkaline soil which contained sand (34.1%), silt (29.5%), and clay (36.4%) was obtained from a local field in Karaj. Physico-chemical properties of the soils are shown in Table 1. Both the acidic and alkaline soils were sampled at a depth of 0–30 cm, air-dried, sieved, and used in greenhouse experiments. Nano-fertilizers and TSP were mixed with the culture media before planting. None of the nanofertilizers were subjected to sonication before applying. N and K fertilizers were also added to the soils before planting at the rates of 120 mg/kg and 85 mg/kg, respectively. The P treatments were applied at a rate of 0 mg/kg (control) or 100 mg/kg.

Preparation of HAP-HA

A specific volume of 1 g/L HA solution was added to 0.2 g of calcium hydroxide and stirred for 4 h at room temperature. Then, 3.2 mL of phosphoric acid (0.5 M) was added drop-wise to the mixture. After 1 h, the reaction mixture was centrifuged, the black precipitate was washed several times to complete the removal of free HA, and dried in a vacuum oven at 60 °C. These nanoparticles can be seen in Fig. 1(a-right).

Measurement of HAP(p) and HAP-HA solubility in water

0.1 g of HAP(p) nanoparticles and 0.13 g of HAP-HA nanoparticles that, according to Table 2, contain the same amounts of P were weighed. The same volumes of distilled water (50 mL) were added to them. Then,

these two mixtures were stirred at an agitation speed of 500 rpm overnight. The obtained mixtures were centrifuged at 10,000 rpm for 10 min, and P concentrations were determined in supernatants using Murphy–Riley method [16]. First, color reagent was prepared as follows: 2 g of ammonium molybdate and 0.137 g of potassium antimony tartrate were dissolved in 50 mL of distilled water in separate containers. 1.32 g of ascorbic acid was dissolved in 75 mL of distilled water. 37.5 mL of ammonium molybdate was mixed with 125 mL of 5 N sulfuric acid. Next, the ascorbic acid solution and 12.5 mL of potassium antimony tartrate solution were added to this solution and the obtained solution was used as color reagent. Due to the instability of ascorbic acid, the reagent solution was prepared fresh to prevent ascorbic acid degradation. Potassium dihydrogen phosphate was used to prepare standard solutions in the P concentration range of 0.08–1 ppm. To measure P concentrations, 5 mL of standards, 5 mL of samples, and 5 mL of blank were separately pipetted into 10-mL volumetric flasks. Next, 1 mL of fresh color reagent was added to each mixture, the obtained solutions were diluted to the mark with distilled water, and mixed. After 10 min, when the color of the solutions changed to blue, the absorptions of the standards and samples were determined using UV–Vis spectroscopy at 882 nm. After that, the absorptions of standard solutions were plotted against standard concentrations, line equation was obtained using the Excel software, and the concentrations of the samples were determined using the line equation.

Preparation of fluorescently tagged HAP nanoparticles

To investigate the existence of HAP nanoparticles in plant using CLSM, HAP(p) nanoparticles were labeled with the fluorescent dyes of ARS and FITC. To synthesize ARS-labeled nanoparticles, a certain amount of ARS was dissolved in sodium hydroxide solution. Next, this solution was added to HAP(p) nanoparticles and this was followed by stirring for 1 h at room temperature. Finally, the mixture was centrifuged several times for the complete removal of free ARS and dried in a vacuum oven at 60 °C [17, 18]. FITC-tagged nanoparticles were synthesized according to previous reports. In brief, amine-functionalized HAP(p) nanoparticles were prepared using APTES. The obtained mixture was centrifuged, washed, dried and then reacted with FITC solution [19, 20]. To visualize nanoparticles in plant using CLSM, wheat seedlings were removed from the soil 1 month after planting and were placed in hydroponic media containing labeled nanoparticles. After 1 week, the seedlings were removed from the hydroponic media, washed with distilled water several times, and fluorescence emissions were investigated in treated and control plants by CLSM at excitation/emission wavelengths of 495/518 nm and 546/590 nm for FITC and ARS, respectively.

Investigation of the distribution and concentration of P in wheat

To investigate the P amounts in different parts of the plant, the wheat plants cultivated in the mixture of peat moss and perlite were used. After harvesting, wheat plants were dried at room temperature for 1 week. Different parts of wheat (i.e., roots, shoots, leaves, and spikes) were separated. 0.2 g of each part was weighed and digested with concentrated nitric acid. Then, digested samples were filtered and diluted with deionized water to 50 mL, and P concentrations in the samples were measured by ICP-AES instrument.

Germination test conditions

Germination experiments were carried out using 5 treatments including HAP(s), HAP(p), blank, TSP, and HAP-HA. The P amounts in HAP formulations and TSP were measured using the vanado-molybdate method [21] before germination test because the fertilizers were intended to be used in quantities containing the same amounts of P. To measure P amounts, first 0.1 g of HAP(p) nanoparticles, 0.1 g of HAP-HA nanoparticles, 0.1 g of TSP, and also 10 mL of HAP(s) nanoparticles were dissolved in 10 mL of concentrated nitric acid and diluted to 50 mL with distilled water. Next, color reagent was prepared. To do so, 5 g of ammonium molybdate was dissolved in 100 mL of distilled water at 50 °C. Then, 0.25 g of ammonium vanadate was dissolved in 75 mL of boiling distilled water and cooled. After that, 35 mL of concentrated nitric acid was gradually added to this solution as it was being stirred. Next, the ammonium molybdate solution was gradually added to the acidic ammonium vanadate solution with stirring. The solution was diluted to 250 mL with distilled water and was used as color reagent. Standard P solutions were prepared using high purity potassium dihydrogen phosphate in the range of 80–800 ppm P. To analyze P using the vanado-molybdate method, 5 mL of standard solutions, 5 mL of blank and 5 mL of fertilizer samples were separately pipetted into 100 mL volumetric flasks, 45 mL of distilled water and 25 mL of color reagent were added, respectively, and, finally, they were diluted to the mark with distilled water and mixed. After 20 min, when the color of the standards and samples changed to yellow, the absorptions of the standards and samples were determined at 470 nm using UV–Vis spectroscopy. Then, the absorptions of the standard solutions were plotted against standard concentrations. Line equation was obtained using the Excel software, and the P concentrations in the fertilizer samples

were calculated using the line equation. The amounts of P in the fertilizers are given in Table 2.

To do germination, 8 healthy wheat seeds of almost the same size were placed in petri dishes on pieces of filter paper. Then, 5 mL of different solutions including HAP formulations, TSP and blank were added in each petri dish. Powder nanoparticles were dispersed in deionized water by ultrasonic homogenizer for 30 min (160 W, 35 kHz) before being added to petri dishes. Three different concentrations of P (i.e., 300, 650, and 1300 ppm) were investigated in germination. Petri dishes were covered and incubated in a dark place for 4 days. Then, root and shoot lengths, root and shoot dry weights, and germination index (GI) were accurately measured. GI was calculated according to the research paper conducted by Gouider et al. [22] as follows:

$$\mathrm{GI} = \frac{\text{The number of germinated seeds in sample}}{\text{Number of germinated seeds in control}} \times \frac{\text{average of root lengths in sample}}{\text{average of root lengths in control}} \times 100.$$

A seed was considered as germinated when root length was at least 5 mm [22].

Data analysis

The experiments were conducted in a completely randomized design with four replications. All data were statistically analyzed using the SAS 9.1 software. Means were compared using the LSD (least significant differences) test at the significance level of 0.05. All the charts were prepared using the Excel software.

Results and discussion

Synthesis of HAP(s) and HAP(p) nanoparticles and their characterization

A number of synthesis methods including sol–gel [23], solid-state methods [24], biosynthesis [25], and wet chemical precipitation [26] have been used to prepare HAP nanoparticles. The most common method for the synthesis of HAP nanoparticles is wet chemical precipitation method thanks to its high repeatability and being easy [26]. In this method, the calcium solution is added to phosphate ions in a stoichiometric ratio of 1.67 to precipitate HAP nanoparticles. This method is performed either via reaction 1 (R_1) or reaction 2 (R_2) as follows:

$$R_1 \quad 10\,\mathrm{Ca(OH)_2} + 6\mathrm{H_3PO_4} \rightarrow \mathrm{Ca_{10}(PO4)_6(OH)_2} + 18\mathrm{H_2O}$$

$$R_2 \quad 10\,\mathrm{Ca(NO_3)_2} + 6\,(\mathrm{NH_4})_2\mathrm{HPO_4} + 8\mathrm{NH_4OH} \rightarrow \mathrm{Ca_{10}(PO4)_6(OH)_2} + 20\,\mathrm{NH_4NO_3} + 6\mathrm{H_2O}$$

R_1 is advantageous over R_2 as it does not have any by-product except water. Thus, the need for frequent washing of the product is eliminated, which makes product separation easy. Moreover, unlike R_2, there is no need for pH adjustment in R_1. For these reasons, the preparation of nanoparticles in R_1 is faster than in R_2. In this study, HAP nanoparticles were synthesized through R_1. This reaction was performed at room temperature. In R_1, low temperatures cause the formation of HAP nanoparticles with less crystallinity [26]. The particles with low crystallinity are more suitable to use as a fertilizer where low crystallinity may help them to dissolve better in soil. Furthermore, the chemicals used in the synthesis method are nontoxic, inexpensive, and available, which makes the method suitable for large-scale production.

To confirm the formation of pure HAP nanoparticles, the synthesized nanoparticles were subjected to FT-IR and XRD analyses. Figure 1b shows the FT-IR spectrum of HAP(p) nanoparticles. FT-IR indicated the characteristic peaks of HAP nanoparticles that were in agreement with other published data [26, 27]. The wide peak at 3400 cm^{-1} is associated with surface adsorbed water molecules [28, 29]. The presence of adsorbed water was also confirmed by bending vibrations at 1640 cm^{-1} [26, 27, 30, 31]. The peak at 3564 cm^{-1} is ascribed to vibrations of OH^- ions [27, 29]. The peaks in the range of 1000–1100 cm^{-1} are attributed to antisymmetric stretching vibrations of P–O band [28]. O–P–O bending vibrations are observed at 566 and 603 cm^{-1} [32]. The peak at 962 cm^{-1} is assigned to PO symmetric vibration [28]. Characteristic peaks of carbonate ions are observed at 1420, 1458, and 876 cm^{-1} [27, 33]. These peaks are formed as a result of atmospheric carbon dioxide entering the reaction during the synthesis of nanoparticles and carbonate substitution in HAP structure (mainly carbonate for phosphate) [26]. This makes the amount of Ca/P molar ratio, which is theoretically 1.67 in HAP nanoparticles, less than 1.67. Most of the studies on HAP synthesis have reported the presence of carbonate ions using FT-IR experiments [26, 27, 33]. However, few articles have measured the amounts of Ca/P ratio and carbon percentage of synthesized HAP nanoparticles. Marchiol et al. reported the Ca/P ratio of 1.60 and the carbonate amount of 0.68% for synthesized HAP nanoparticles [10]. In another study, Levinskas et al. reported the amounts 1.66% and 0.86% for Ca/P ratio and carbon dioxide, respectively, in commercial HAP nanoparticles [34]. Also, Priyam et al. reported the Ca/P ratio of 1.58

in the biologically synthesized HAP nanoparticles [35]. In our study, the carbon percentage of HAP(p) nanoparticles was determined using the CHN technique and the obtained value was 0.4%.

Figure 1c, d shows XRD patterns of HAP(p) and HAP(s) nanoparticles, respectively. Two main diffraction peaks of HAP are observed at 2θ degrees of 30° and 37°. According to the literature, they correspond to crystallographic planes (002) and (211) of HAP [14, 36]. Figure 1e shows that X-ray pattern of HAP(p) nanoparticles is in good agreement with the standard XRD data of HAP (JCPDS Card No. 24-0033). Therefore, XRD patterns of nanoparticles showed the formation of crystalline HAP nanoparticles without any extra peak for unreacted reagents and byproducts. Also, the broadening of the peaks confirmed the formation of nanoparticles [1]. The peak with Miller index (211) was merged with the next two peaks with Miller indices (112) and (300), and these peaks were not separated due to peak broadening. The merging of these peaks in HAP nanoparticles has been previously reported [1, 7, 10].

Figure 2 shows TEM images of HAP(s) nanoparticles (a, b) and SEM images of HAP(p) nanoparticles (c, d). The images indicated the formation of nano-size particles and their rod-like shapes. Average sizes of the particles were calculated using the ImageJ program and were found to be 8 ± 2.02 nm and 27 ± 6 nm for HAP(s) nanoparticles and HAP(p) nanoparticles, respectively. In each sample, 100 particles were selected randomly from several pictures.

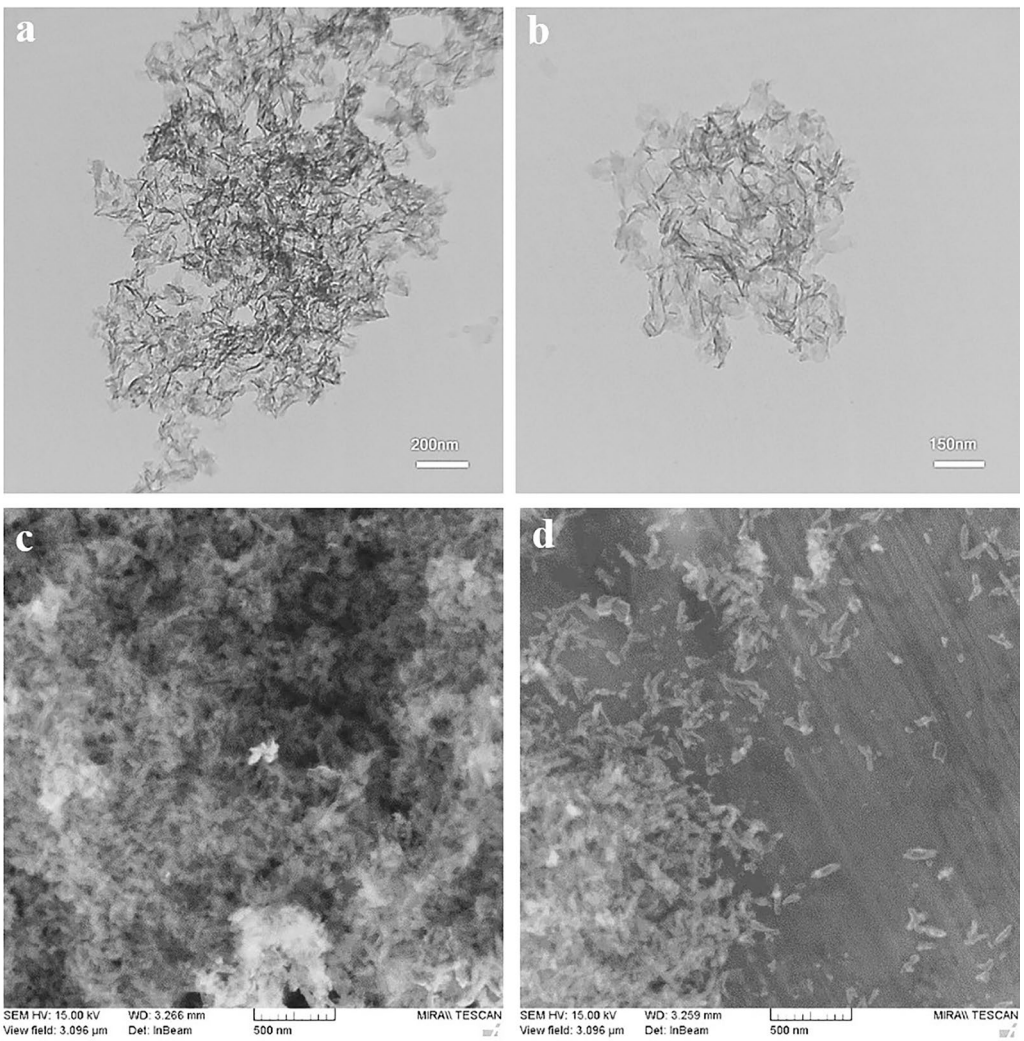

Fig. 2 TEM images of HAP(s) nanoparticles (**a**, **b**). SEM images of HAP(p) nanoparticles (**c**, **d**). Abbreviations: HAP(p), hydroxyapatite nanoparticles in powder form. HAP(s), hydroxyapatite nanoparticles in suspension form

Preparation and characterization of HAP-HA

Humic acids (HA) are a class of complex organic materials that are found in natural aquatic and soil systems. They play an important role in soil fertility and plant nutrition, and promote crop yield [37]. In the present study, HAP-HA nanoparticles were prepared to assess the effect of HA on fertilizing properties of HAP nanoparticles. Figure 3 shows UV–Vis spectra of HA solution and the supernatant of HAP-HA nanoparticles. The latter is the upper solution obtained from centrifuging HAP-HA nanoparticles. It was observed that the HA solution had a high absorption value. However, UV–Vis absorption spectrum of the supernatant of HAP-HA nanoparticles showed a dramatic decrease in absorption value, which was indicative of HA adsorption on the surface of HAP nanoparticles. To quantify HA adsorption, the carbon amounts of HAP-HA and HAP(p) nanoparticles were measured using the CHN technique. The carbon contents were found to be 8% and 0.4%, respectively. The low carbon content of HAP(p) is due to atmospheric carbon dioxide as mentioned earlier in the part explaining FT-IR spectrum of the HAP(p) nanoparticles. Also, it was observed (Fig. 4a) that functionalization with HA did not change the XRD pattern of HAP nanoparticles, as previously reported by Wang et al. [27]. The AFM image of HAP-HA nanoparticles given in Fig. 4b shows that the particles are spherical and that their average size is 13.7 nm ± 4.2.

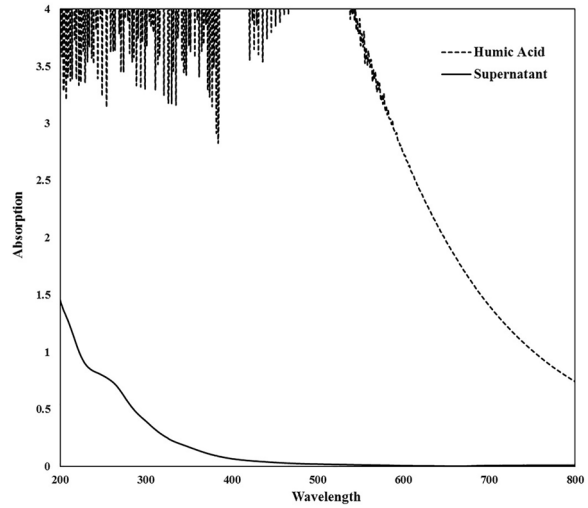

Fig. 3 UV–Vis spectra of HA and the supernatant of HAP-HA nanoparticles. Abbreviations: HA, humic acid; HAP-HA, humic acid-modified hydroxyapatite nanoparticles

Detection of nanoparticles in plant using microscopy techniques

To visualize the uptake of nanoparticles in plant, CLSM and TEM were used. The CLSM images of both the ARS- and FITC-labeled nanoparticles (Figs. 5, 6) showed the presence of HAP(s) nanoparticles in the root and stem of the treated plant, whereas the nanoparticles were not observed in the blank. TEM images of the plant root treated with HAP(s) nanoparticles (Fig. 7) revealed the presence and accumulation of nanoparticles in apoplast and symplast. The presence of different nanoparticles in apoplast and symplast has been previously explained [9, 38]. Some papers have reported the existence of HAP nanoparticles in the roots and stems of plants. In 2018,

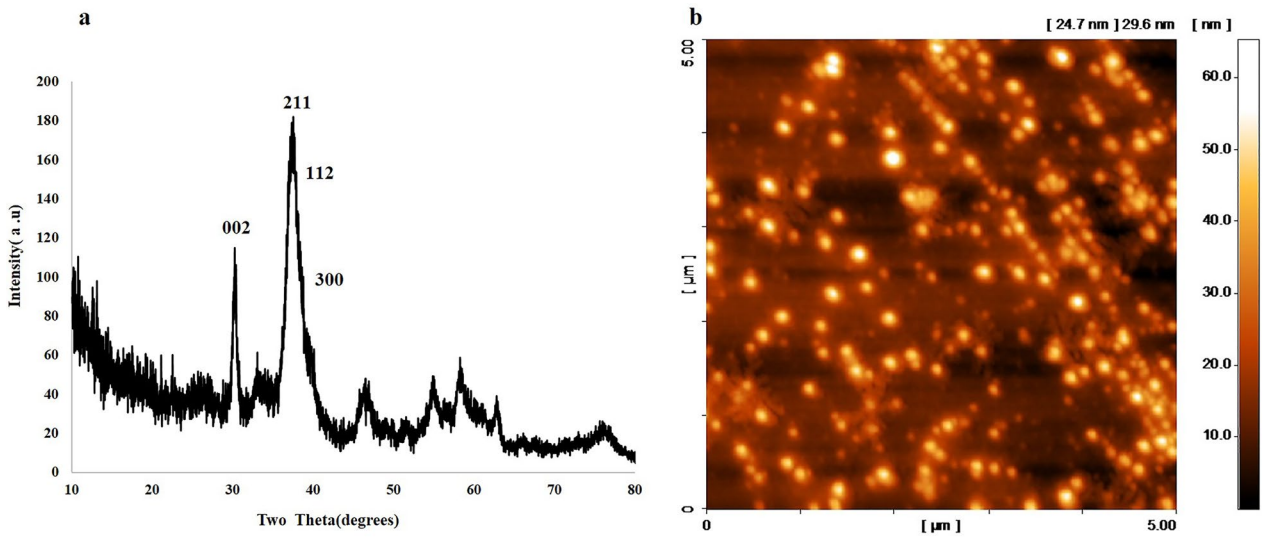

Fig. 4 XRD pattern of HAP-HA nanoparticles (**a**). AFM image of HAP-HA nanoparticles (**b**). Abbreviation: HAP-HA, humic acid-modified hydroxyapatite nanoparticles

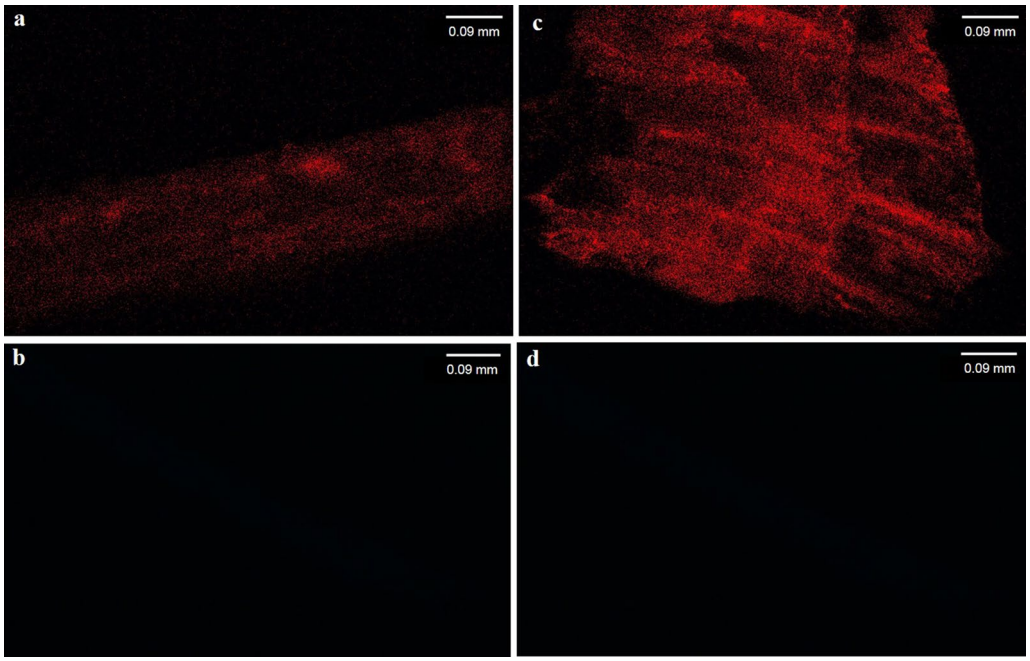

Fig. 5 CLSM images of ARS-labeled HAP nanoparticles. This figure shows the plant root treated with ARS-labeled HAP nanoparticles (**a**), the root of the blank sample (**b**), the plant shoot treated with ARS-labeled HAP nanoparticles (**c**), and the shoot of the blank sample (**d**). Imaging was performed at excitation/emission wavelengths of 546/590 nm. Abbreviations: ARS, alizarin red S; HAP, hydroxyapatite nanoparticles

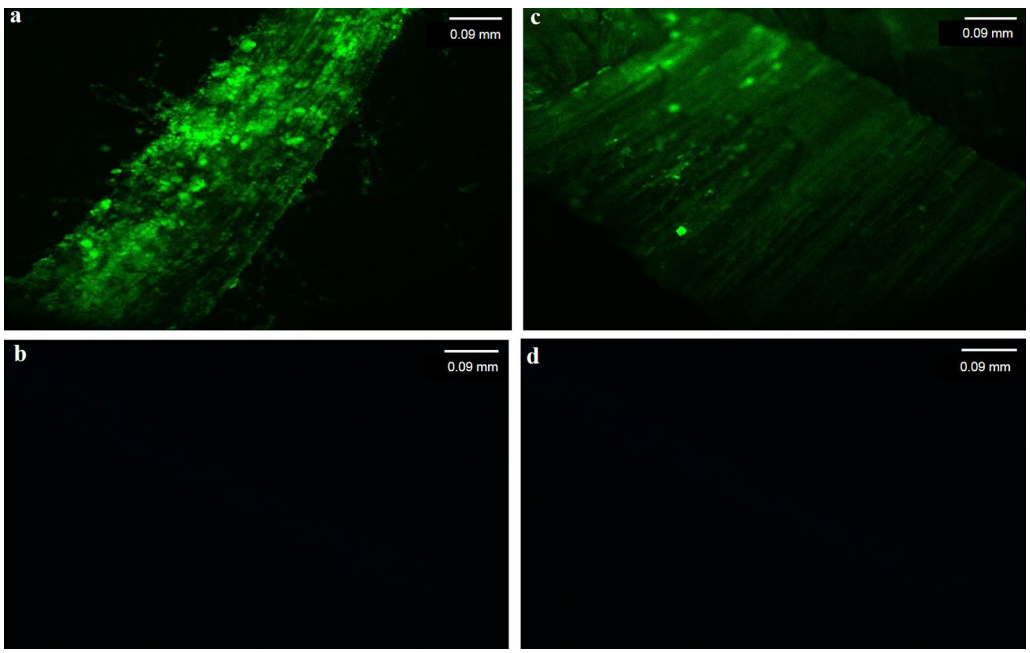

Fig. 6 CLSM images of FITC-labeled HAP nanoparticles. This figure shows the plant root treated with FITC-labeled HAP nanoparticles (**a**), the root of the blank sample (**b**), the plant shoot treated with FITC-labeled HAP nanoparticles (**c**), and the shoot of the blank sample (**d**). Imaging was performed at excitation/emission wavelengths of 495/518 nm. Abbreviations: FITC, fluorescein isothiocyanate; HAP, hydroxyapatite nanoparticles

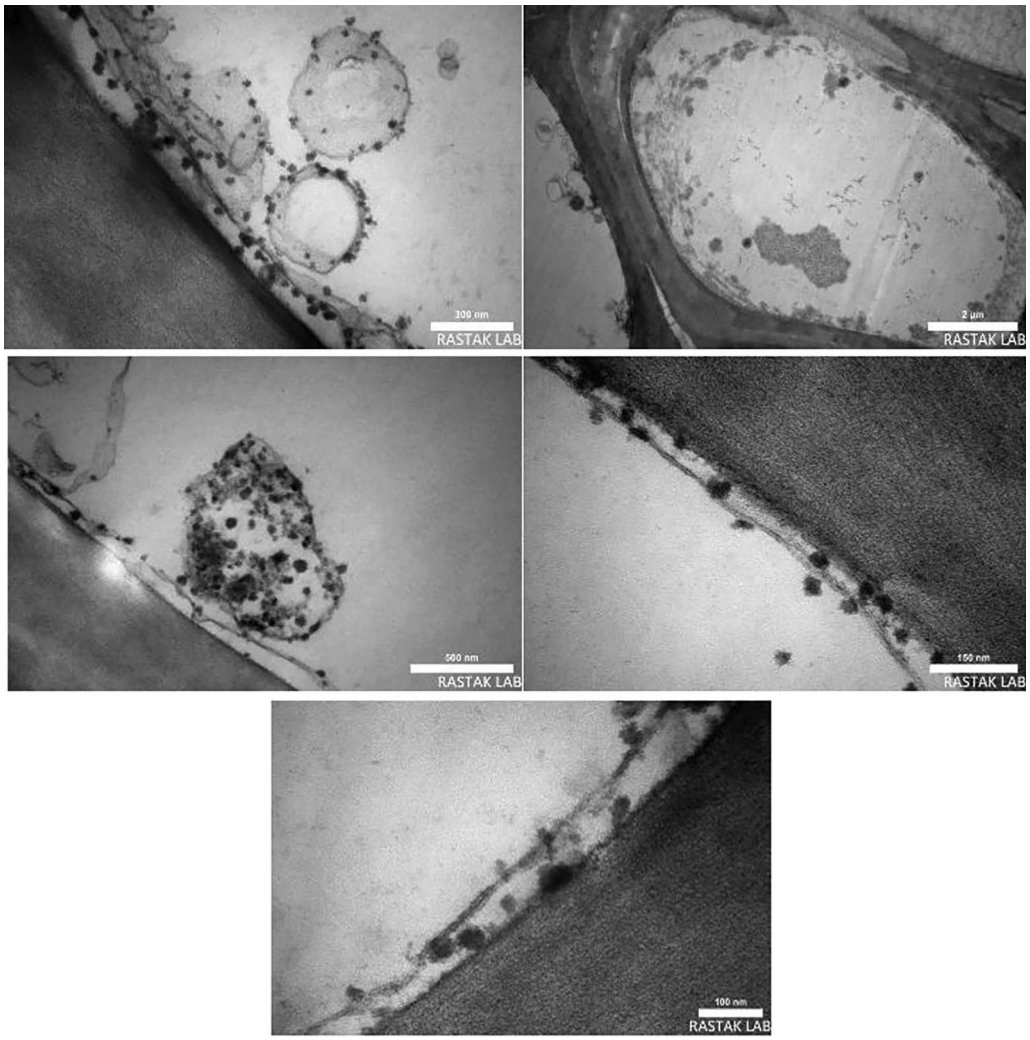

Fig. 7 TEM images of HAP nanoparticles in wheat root. Abbreviation: HAP, hydroxyapatite nanoparticles

a group of researchers studied the use of HAP nanoparticles in Pb immobilization and reduction of Pb uptake in rice. TEM images of plant cells exposed to HAP nanoparticles in hydroponic medium showed the presence and the uptake of nanoparticles in root cells [36]. In another study, the effect of HAP nanoparticles on chickpea *(Cicer arietinum)* germination was investigated. TEM images confirmed the presence and accumulation of nanoparticles in plant stem [39]. In the study conducted by Szameitat et al., in which the interaction of barley roots with HAP nanoparticles was investigated, TEM analysis confirmed the presence of nanoparticles in roots. Szameitat et al. concluded that HAP nanoparticles first penetrated the roots via apoplast of mature epidermal and cortical cells and then dissolved there due to the acidic properties of cell wall, and that orthophosphate ions were translocated towards aboveground parts of the plant [3]. However, this study [3] was performed in hydroponic medium, and the interactions between soil and HAP nanoparticles were not considered. Thus, the results may not be generalizable to the soil environment.

Investigation of the distribution and uptake of P in wheat

Table 3 shows the uptake and distribution of P in different parts of wheat under the treatments of blank, HAP(s), and TSP. The higher P amounts in different parts of the plant treated with HAP nanoparticles than in the blank sample confirmed the uptake of HAP nanoparticles. For example, the amount of P in the spike of the plant treated with HAP nanoparticles was 2.8 times larger than the P amount in the blank sample. Also, it was found that the highest amounts of P were available in spikes in both the TSP and HAP treatments as expected. The comparison of P amounts in TSP and HAP treatments showed higher P contents in TSP treatment in all plant parts. This result was probably because of TSP's high solubility which led

Table 3 P amounts in different parts of wheat plant in blank, HAP(s) and TSP treatments

Sample name	P amount (mg/kg)
Root-blank	666.66
Shoot-blank	306.45
Leaf-blank	156.25
Spike-blank	865.38
Root-HAP	1037.37
Shoot-HAP	796.4
Leaf-HAP	1043.47
Spike-HAP	2439.21
Root-TSP	1652.63
Shoot-TSP	1486.48
Leaf-TSP	2813.18
Spike-TSP	3431.29

P, phosphorus; HAP(s), hydroxyapatite nanoparticles in suspension form; TSP, triple super phosphate

to higher uptake in the plant. This finding was in agreement with that of the study conducted by Montalvo et al. in which P uptake in wheat shoots in HAP treatment was lower than in TSP treatment [5]. Also, our results were consistent with the results of the research study conducted by Xiong et al. where the P uptake in sunflower shoots treated with HAP nanoparticles was lower than in sunflower shoots treated with TSP in alkaline soil. Xiong et al. concluded that the high solubility of TSP caused higher P concentrations in the sunflower shoots treated with TSP [8]. However, few studies have measured the amounts of P uptake in the plants treated with HAP nanoparticles. In the study carried out by Priyam et al., the effect of HAP nanoparticles on tomato growth was investigated. The analysis of P contents in the plants treated with HAP nanoparticles confirmed the P uptake [35]. However, in Priyam et al.'s research, P concentration was not determined in the plants treated with traditional P fertilizers.

Germination test

Statistical analysis confirmed that all treatments had a significant effect on germination ($p < 0.05$). The results of germination test are given in Fig. 8. It was found that when the P concentration was increased, shoot elongation, root elongation, and GI decreased in TSP and HAP(s) treatments. In contrast, no significant difference was found in HAP(p) and HAP-HA treatments with an increase in concentration. Also, it was observed that increasing the concentration led to a decrease in shoot weight in HAP(s) and TSP treatments. The above-mentioned increase in concentration also led to an increase in shoot weight in HAP(p) treatment. Moreover, when the P concentration was increased, a statistically significant decrease in root weight was observed in HAP(s) and TSP treatments whereas slight increases were observed in HAP(p) and HAP-HA treatments. Overall, it can be said that unlike HAP(p) and HAP-HA treatments, HAP(s) and TSP treatments were highly affected by concentration, i.e., a decrease in responses was observed as a result of the increase in concentration, which indicated toxicity in higher concentrations. This may be due to the increase in diffusion and uptake of nanoparticles in seeds, which is related to the fact that HAP(s) nanoparticles are in a suspension form and that TSP is water-soluble. Furthermore, the lowest responses were obtained for TSP treatment. It should be said that the responses in TSP treatment were even less than those of the blank except shoot weight and GI in the P concentration of 300 ppm. Similarly, the investigation of the effect of HAP nanoparticles on tomato seed germination explained that germination parameters in traditional fertilizer treatment were significantly lower than in HAP treatment and even lower than in blank treatment [35]. Most studies on HAP toxicity in plants have shown concentration-dependent toxicity. However, in these studies, the toxicity of HAP nanoparticles was not compared with that of traditional P fertilizers. A group of researchers studied the toxicity of HAP nanoparticles on cucumber germination. It was found that GI and germination percentage increased rapidly up to a P concentration of 1000 mg/L. Nevertheless, in higher concentrations, inhibitory effects were observed on shoot and root growth [40]. In another study by Marchiol et al., the effect of HAP nanoparticles (in the P concentration of 2–2000 mg/L) on tomato germination was investigated [10]. The results demonstrated that germination percentage did not depend on concentration, whereas root elongation significantly increased as a result of an increase in concentration. The investigation of the toxicity of HAP nanoparticles in chickpea revealed that the highest value of GI was obtained in a concentration of 1000 mg/L and higher concentrations led to a significant inhibition of plant growth [39].

Fertilizers efficiency in different culture media

According to the literature, in most of the studies, the efficiency of HAP nanoparticles has been investigated only in one culture medium. In fact, few studies have evaluated the effect of different culture media on the fertilizing properties of HAP nanoparticles. In 2022, researchers investigated HAP's fertilizing effects on tomato growth in three artificial soils containing vermiculite, perlite, and peat moss. The pH of these media was manually adjusted to prepare the culture media with acidic, neutral, and alkaline pHs. The results demonstrated the fertilizing potential of HAP nanoparticles in all the three media

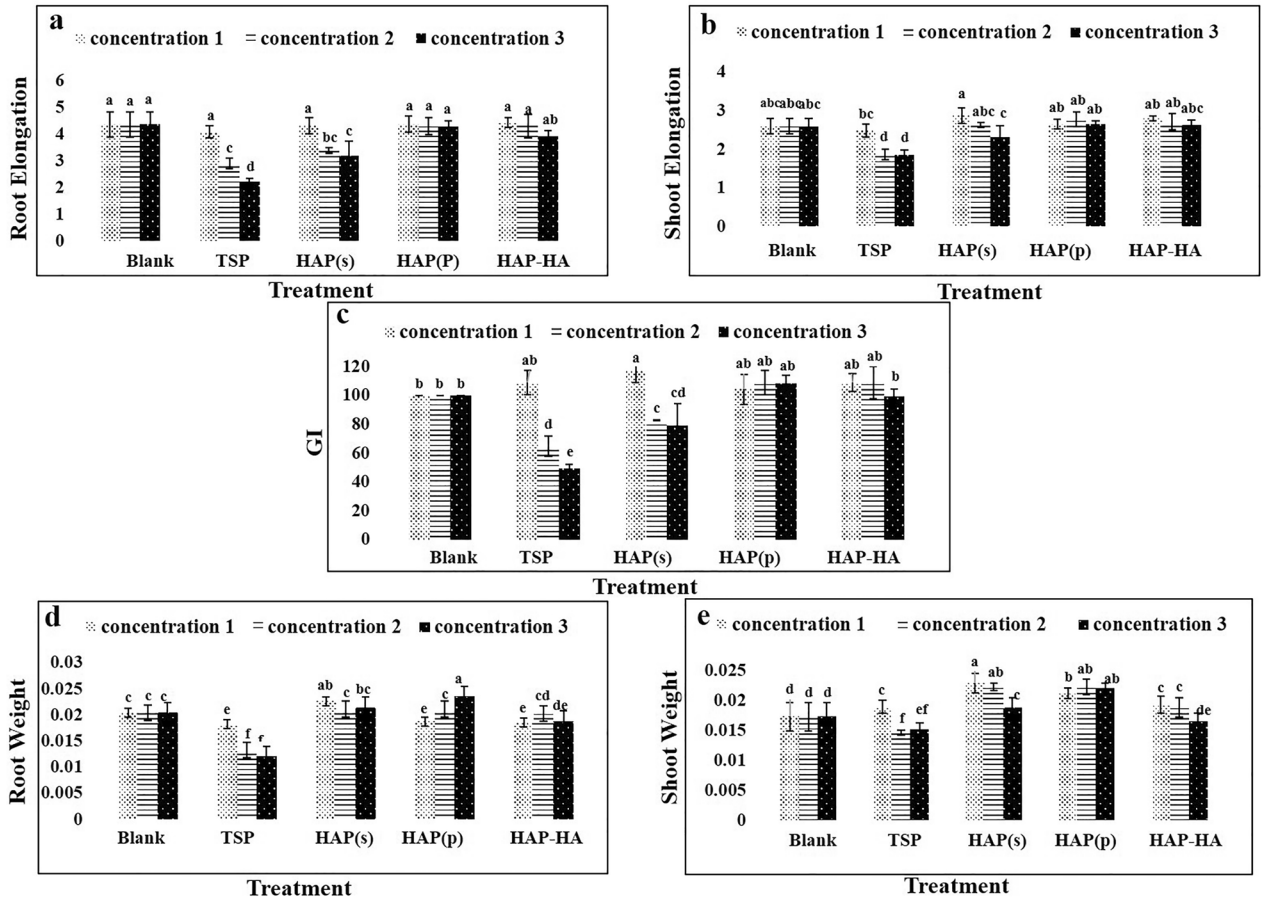

Fig. 8 Germination experiment. The effect of nanoformulations and TSP on root elongation (**a**), shoot elongation (**b**), GI (**c**), root dry weight (**d**), and shoot dry weight (**e**) in three P concentrations. Different letters indicate statistically significant differences between treatments ($p < 0.05$). Abbreviations: TSP, triple super phosphate; HAP(s), hydroxyapatite nanoparticles in suspension form; HAP(p), hydroxyapatite nanoparticles in powder form; HAP-HA, humic acid-modified hydroxyapatite nanoparticles; GI, germination index; P, phosphorus

[35]. However, because of using artificial soils, the results of the above-mentioned study cannot likely be generalizable to natural soils. Also, in another study, the effect of HAP nanoparticles on sunflower growth was assessed in two soils: one acidic and the other alkaline [8]. In our study, the efficiency of the synthesized HAP nanoparticles was investigated in four different culture media, i.e., the mixture of peat moss and perlite, cocopeat, acidic soil, and alkaline soil.

Fertilizers efficiency in the mixture of peat moss and perlite

As shown in Fig. 9a, b, the measured variables including aboveground weight and spike weight in HAP(s) treatment were significantly higher than those of the blank, which shows the fertilizing properties of HAP(s) nanoparticles. Aboveground weights and spike weights were compared in HAP(s) and TSP treatments, but no significant differences were observed between them. The images of wheat pots and spikes (Fig. 9c, d) confirmed the above-mentioned results. A study on the effects of HAP nanoparticles on soybean culture in the mixture of peat moss and perlite showed that the efficiency of HAP nanoparticles was significantly higher than that of traditional P fertilizer, in such a way that growth rate increased by 32% in HAP treatment compared to the traditional fertilizer [7].

Fertilizers efficiency in cocopeat medium

Figure 10 shows the fertilizing effects of HAP formulations and TSP in cocopeat medium. The comparison of the two variables of spike weight and aboveground weight in HAP treatments and blank indicates fertilizing properties of HAP nanoparticles. In addition, Fig. 10 indicates that there is a significant difference between HAP treatments and TSP, which in turn demonstrates higher fertilizing effects of HAP formulations. For example, aboveground weight and spike weight in HAP-HA treatment in cocopeat medium were 45.51% and 45.05%

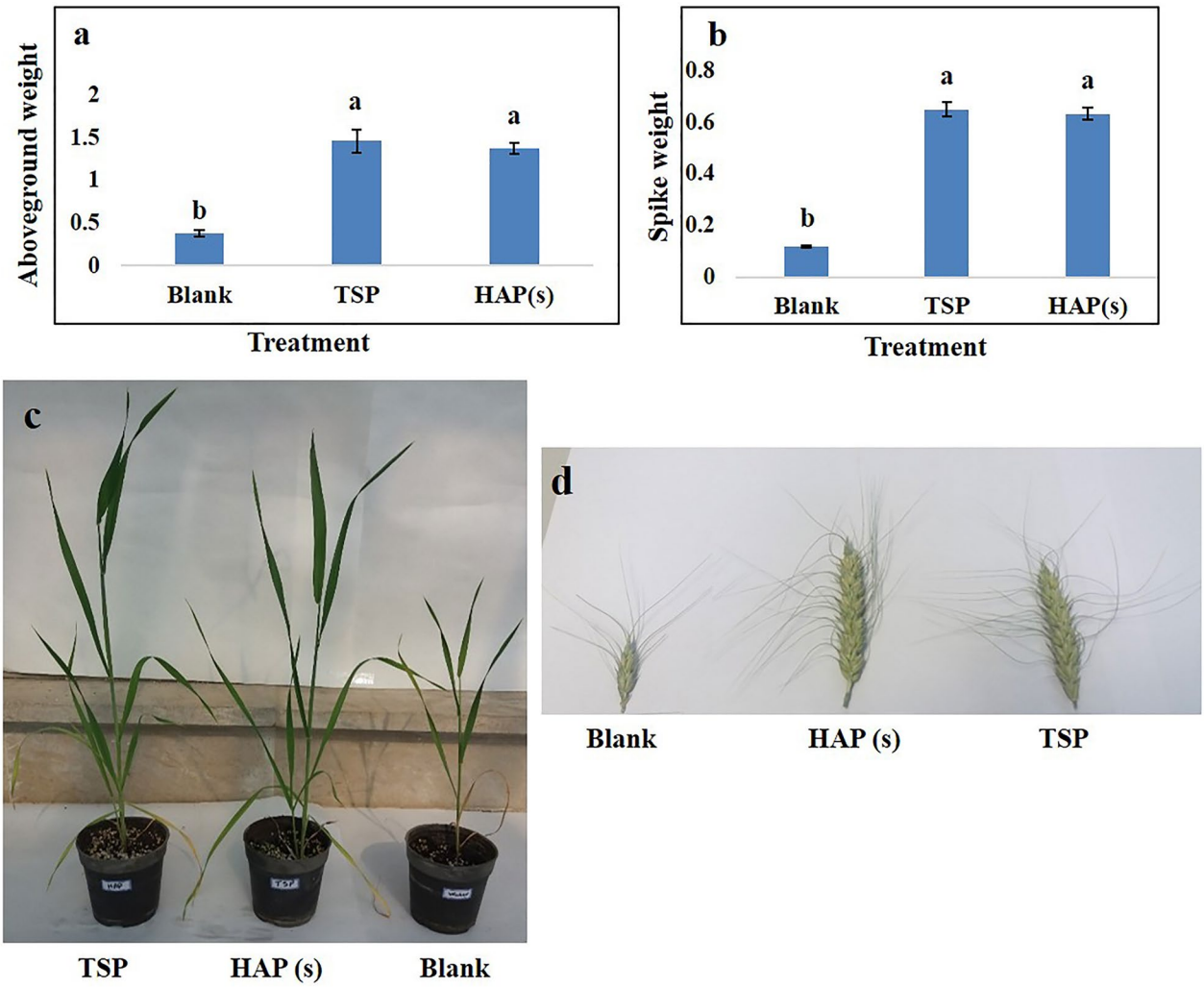

Fig. 9 Fertilizing effects of HAP(s) nanoparticles and TSP on wheat growth in the mixture of peat moss and perlite. This figure shows the effect of treatment on aboveground weight (**a**), the effect of treatment on spike weight (**b**), the growth of wheat plants 4 weeks after germination under the treatments of HAP(s), TSP, and blank in greenhouse (**c**), and the images of spikes in blank, TSP, and HAP(s) treatments (**d**) in the mixture of peat moss and perlite. Different letters indicate statistically significant differences between treatments ($p < 0.05$). Abbreviations: TSP, triple super phosphate; HAP(s), hydroxyapatite nanoparticles in suspension form

higher than those of TSP treatment. Figure 10 also shows the fertilizing properties of HAP-HA nanoparticles and that there are no significant differences between HAP(s), HAP(p), and HAP-HA. To the best of our knowledge, this study is the first report on fertilizing properties of HAP-HA nanoparticles.

Fertilizers efficiency in acidic and alkaline soils

Comparing spike weights and aboveground weights of HAP formulations and TSP in acidic soil (Fig. 11) revealed that the efficiency of HAP formulations was higher than that of TSP. Furthermore, there were no significant differences between HAP formulations including HAP(s), HAP(p), and HAP-HA. In 2015, researchers investigated the effect of HAP nanoparticles on wheat growth in two acidic soils. The results of the study indicated that the fertilizing properties of HAP nanoparticles were significantly less than those of TSP. Also, the study revealed that plant growth improved in the soil with lower pH. The authors attributed this effect to the better solubility of HAP nanoparticles in higher acidity [5].

Figure 12 shows that the fertilizing properties of TSP are significantly higher than those of nanoformulations in alkaline soil. For example, aboveground weight and spike weight in the TSP treatment were 35.18% and 50.52% higher than those of HAP-HA treatment. This finding is consistent with the findings of the study conducted by Xiong et al. where they observed that HAP nanoparticles

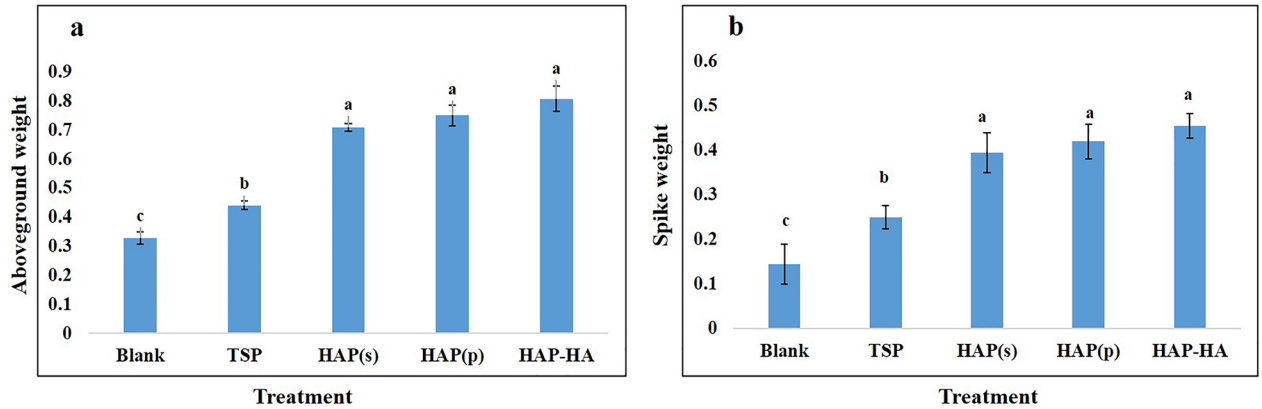

Fig. 10 Fertilizing effects of nanoformulations and TSP on wheat growth in cocopeat medium. This figure shows the effects of different treatments on aboveground weight (**a**) and spike weight (**b**) in cocopeat medium. Lowercase letters indicate statistically significant differences at $p < 0.05$. Abbreviations: TSP, triple super phosphate; HAP(s), hydroxyapatite nanoparticles in suspension form; HAP(p), hydroxyapatite nanoparticles in powder form; HAP-HA, humic acid-modified hydroxyapatite nanoparticles

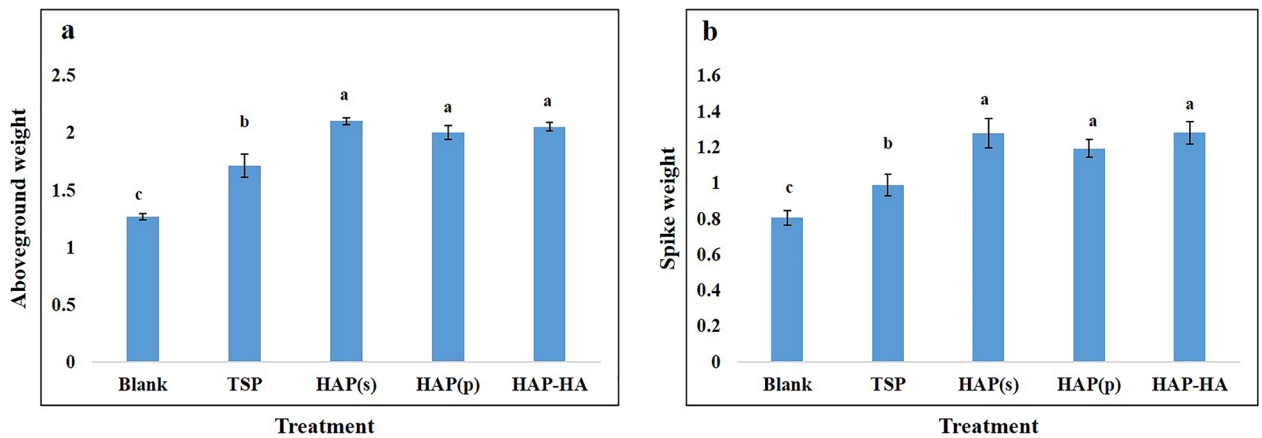

Fig. 11 Fertilizing effects of nanoformulations and TSP on wheat growth in acidic soil. This figure shows the effects of different treatments on aboveground weight (**a**) and spike weight (**b**) in acidic soil. Lowercase letters indicate statistically significant differences ($p < 0.05$). Abbreviations: TSP, triple super phosphate; HAP(s), hydroxyapatite nanoparticles in suspension form; HAP(p), hydroxyapatite nanoparticles in powder form; HAP-HA, humic acid-modified hydroxyapatite nanoparticles

remarkably improved sunflower growth in an acidic soil while no significant fertilizing properties were observed in alkaline soil [8]. In another study carried out by the same group, when two acidic and alkaline soils were incubated with HAP nanoparticles, it was found that P availability in acidic soil was higher than in alkaline soil [4]. As a result, they hypothesized that because of the higher solubility of HAP nanoparticles at low pHs, nanoparticles may have dissolved in soil and orthophosphate ions may have been absorbed by the plant. In our study, microscopy analyses confirmed the presence of nanoparticles in the root and stem of the plant, which can be indicative of nanoparticles uptake by the plant. In contrast, based on the results mentioned above, in acidic media, i.e., the mixture of peat moss and perlite, cocopeat, and acidic soil, HAP nanoparticles showed a high fertilizing effect, whereas in alkaline soil a slight fertilizing property was observed. This shows that nanoparticles were likely dissolved in soil and that, instead of nanoparticles, phosphate ions were absorbed by the plant. These conflicting results in our study may have occurred because the HAP nanoparticles were absorbed by the plant via both the direct absorption of nanoparticles by the roots and uptake of phosphate ions resulting from HAP dissolution in culture media. However, the results of our efficiency tests along with the findings of the above-mentioned studies [4, 8] show that the main mechanism of P uptake in the plants treated with HAP nanoparticles is probably

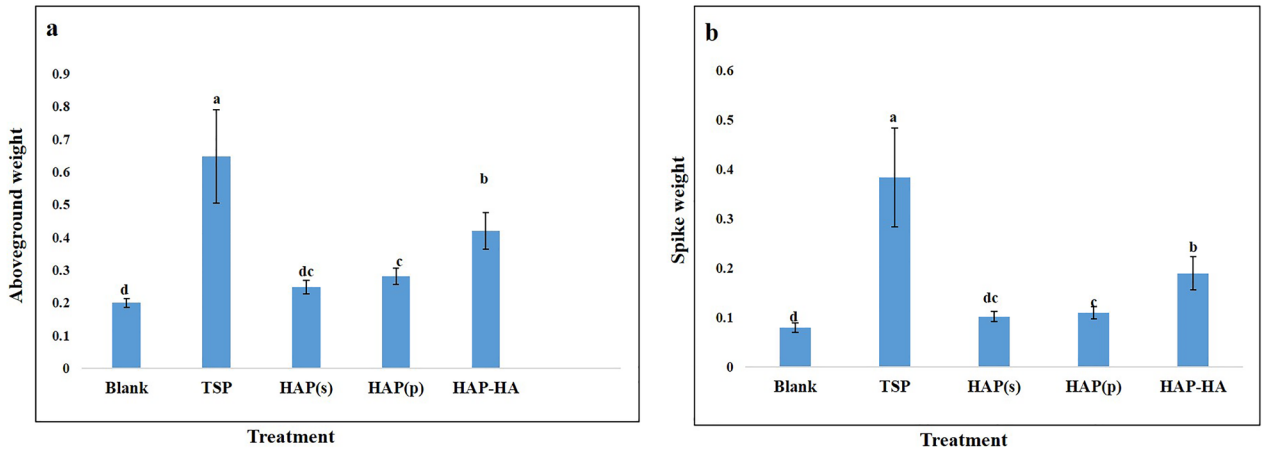

Fig. 12 Fertilizing effects of nanoformulations and TSP on wheat growth in alkaline soil. This figure shows the effects of different treatments on aboveground weight (**a**) and spike weight (**b**) in alkaline soil. Lowercase letters indicate statistically significant differences at $p < 0.05$. Abbreviations: TSP, triple super phosphate; HAP(s), hydroxyapatite nanoparticles in suspension form; HAP(p), hydroxyapatite nanoparticles in powder form; HAP-HA, humic acid-modified hydroxyapatite nanoparticles

the dissolution of P in soil and its absorption in the phosphate form.

In our study, the results obtained from efficiency tests in acidic and alkaline media can be explained according to Ca/P ratio in calcium phosphate compounds in the following way: It is well-known that the solubility of calcium phosphates depends on their Ca/P ratio [41]. The lower the Ca/P molar ratio, the more water-soluble and acidic the calcium phosphate compound. Thus, calcium dihydrogen phosphate (Ca/P ratio of 0.5) that is the the main component of the TSP fertilizer is the most acidic and water-soluble calcium phosphate and HAP (Ca/P ratio of 1.67) is the most alkaline and water-insoluble [41, 42]. In our study, HAP nanoparticles showed higher efficiency in acidic media because, according to the facts mentioned above, they are alkaline. Hence, despite their very low solubility in water, they are soluble in acidic media and their solubility in acidic media is more than in alkaline media, while TSP is highly acidic, and as a result, dissolves in alkaline media more than in acidic ones.

The results of our study in alkaline soil also showed higher efficiency of HAP-HA nanoparticles compared to that of HAP(s) nanoparticles and HAP(p) nanoparticles in a way that aboveground weight and spike weight in HAP-HA treatment were 33% and 42% higher than those of HAP(p) treatment. This may have occurred for two reasons. First, according to the solubility tests, the solubility of HAP-HA nanoparticles was higher than that of HAP nanoparticles. The concentrations of soluble P were 0.4 ppm and 0.7 ppm in HAP(p) and HAP-HA nanoparticles, respectively. As a result, more soluble P may have been absorbed by the plant. Second, the dissolution of HAP-HA nanoparticles in soil releases HA, which can in turn improve plant growth. The higher efficiency of HAP-HA nanoparticles compared to other HAP particles may confirm the hypothesis of nanoparticles dissolution in soil and their absorption in the form of phosphate ions. However, the exact mechanism of uptake and translocation of nanoparticles in plants is not yet fully elucidated. To understand this mechanism accurately, a comprehensive quantitative analysis using speciation techniques like X-ray absorption spectroscopy should be performed on different parts of the plant treated with nanoparticles to determine what the structure of P is in different parts of the plant. Also, P speciation should be performed in culture media before planting and after harvesting. The present research study will develop in this direction.

Conclusions

To conclude, it was found that the fertilizing properties of HAP nanoparticles depended on the culture media. In the culture media of cocopeat, the mixture of peat moss and perlite, and acidic soil HAP nanoparticles showed remarkable fertilizing properties comparable with those of TSP as a conventional P fertilizer. However, these nanoparticles showed just a slight fertilizing effect in alkaline soil. This occurs probably because the first three culture media are acidic and HAP nanoparticles dissolve in these media, whereas the solubility of HAP nanoparticles is negligible in alkaline media. This finding may indicate that HAP nanoparticles dissolve in soil before they are absorbed by the plant in the form of nanoparticles. In fact, orthophosphate ions are absorbed by the plant and translocated to the aboveground parts of the plant. However, further research studies are required to confirm this finding. Moreover, this study revealed that

it is not necessary that all formulations be in suspension form to act as a fertilizer. According to the results obtained through our study, powder nanoparticles, i.e., HAP-HA and HAP(p), showed fertilizing effects without the need to convert them to suspension. The inhibitory effects were observed in germination test in high concentrations of P in both HAP formulations and TSP. However, these effects were more significant in TSP in such a way that the lowest values of germination parameters were obtained for TSP. The values of these parameters were even lower than those of the blank.

Abbreviations

ARS	Alizarin red S
AFM	Atomic force microscopy
APTES	3-Aminopropyltriethoxy silane
CMC	Carboxy methylcellulose sodium salt
CLSM	Confocal laser scanning microscopy
FT-IR	Fourier transform infrared
FITC	Fluorescein isothiocyanate
GI	Germination index
HA	Humic acid
HAP(p)	Hydroxyapatite nanoparticles in powder form
HAP(s)	Hydroxyapatite nanoparticles in suspension form
HAP-HA	Humic acid-modified hydroxyapatite nanoparticles
ICP-AES	Inductively coupled plasma-atomic emission spectroscopy
N	Nitrogen
P	Phosphorus
SEM	Scanning electron microscopy
TEM	Transmission electron microscopy
TSP	Triple super phosphate
XRD	X-ray diffraction

Acknowledgements
The authors would like to thank the Nanotechnology Department of Agricultural Biotechnology Research Institute of Iran for their cooperation. The authors would also like to thank Mr. Mohammadreza Noroozi for his assistance in the preparation of the article.

Author contributions
MN designed the project, wrote the manuscript, and performed most of analyses and experiments. LS performed statistical analyses of the data and collaborated on editing the manuscript. LM and KS cooperated in data interpretation and design of some experiments. PH took microscopic images and collaborated on figures preparation. All authors read the manuscript and approved it.

Funding
This study was financially supported by Agricultural Biotechnology Research Institute of Iran (Grant No. 12-05-05-037-97038-971391).

Availability of data and materials
The data that support the findings of this study are available on request from the corresponding author.

Declarations

Ethics approval and consent to participate
Not applicable.

Consent for publication
Not applicable.

Competing interests
The authors declare no competing interests.

Author details
[1]Nanotechnology Department, Agricultural Biotechnology Research Institute of Iran (ABRII), Agricultural Research, Education and Extension Organization (AREEO), Karaj, Iran. [2]Agronomy and Plant Breeding Department, Tehran University, Karaj, Iran. [3]Laboratories Department, Soil and Water Research Institute (SWRI), Agricultural Research, Education and Extension Organization (AREEO), Karaj, Iran.

Received: 8 February 2023 Accepted: 7 July 2023
Published online: 04 August 2023

References

1. Samavini R, Sandaruwan C, De Silva M, Priyadarshana G, Kottegoda N, Karunaratne V. Effect of citric acid surface modification on solubility of hydroxyapatite nanoparticles. J Agric Food Chem. 2018;66:3330–7.
2. Schachtman DP, Reid RJ, Ayling SM. Phosphorus uptake by plants: from soil to cell. Plant Physiol. 1998;116:447–53.
3. Szameitat AE, Sharma A, Minutello F, Pinna A, Er-Rafik M, Hansen TH, et al. Unravelling the interactions between nano-hydroxyapatite and the roots of phosphorus deficient barley plants. Environ Sci Nano. 2021;8:444–59.
4. Xiong L, Wang P, Kopittke PM. Tailoring hydroxyapatite nanoparticles to increase their efficiency as phosphorus fertilisers in soils. Geoderma. 2018;323:116–25.
5. Montalvo D, McLaughlin MJ, Degryse F. Efficacy of hydroxyapatite nanoparticles as phosphorus fertilizer in andisols and oxisols. Soil Sci Soc Am J. 2015;79:551–8.
6. Zhang Z, Chen Y, Mandler D, Shenker M. Transport of hydroxyapatite nanoparticles coated with polyacrylic acid under unsaturated water flow in soil columns. Soil Sci Plant Nutr. 2023;2023:1–13.
7. Liu R, Lal R. Synthetic apatite nanoparticles as a phosphorus fertilizer for soybean (Glycine max). Sci Rep. 2014;4:1–6.
8. Xiong L, Wang P, Hunter MN, Kopittke PM. Bioavailability and movement of hydroxyapatite nanoparticles (HA-NPs) applied as a phosphorus fertiliser in soils. Environ Sci Nano. 2018;5:2888–98.
9. Solanki P, Bhargava A, Chhipa H, Jain N, Panwar J. Nano-fertilizers and their smart delivery system. Nanotechnologies in food and agriculture. London: Springer; 2015. p. 81–101.
10. Marchiol L, Filippi A, Adamiano A, Degli Esposti L, Iafisco M, Mattiello A, et al. Influence of hydroxyapatite nanoparticles on germination and plant metabolism of tomato (*Solanum lycopersicum* L.): preliminary evidence. Agronomy. 2019;9:161.
11. Elsayed AA, Ahmed E-G, Taha ZK, Farag HM, Hussein MS, AbouAitah K. Hydroxyapatite nanoparticles as novel nano-fertilizer for production of rosemary plants. Sci Hortic. 2022;295:110851.
12. Sharma B, Shrivastava M, Afonso LO, Soni U, Cahill DM. Zinc-and magnesium-doped hydroxyapatite nanoparticles modified with urea as smart nitrogen fertilizers. ACS Appl Nano Mater. 2022;5:7288–99.
13. Kottegoda N, Sandaruwan C, Priyadarshana G, Siriwardhana A, Rathnayake UA, Berugoda Arachchige DM, et al. Urea-hydroxyapatite nanohybrids for slow release of nitrogen. ACS Nano. 2017;11:1214–21.
14. Kottegoda N, Munaweera I, Madusanka N, Karunaratne V. A green slow-release fertilizer composition based on urea-modified hydroxyapatite nanoparticles encapsulated wood. Curr Sci. 2011;2011:73–8.
15. Reynolds ES. The use of lead citrate at high pH as an electron-opaque stain in electron microscopy. J Cell Biol. 1963;17:208.
16. Murphy J, Riley JP. A modified single solution method for the determination of phosphate in natural waters. Anal Chim Acta. 1962;27:31–6.
17. Misra D. Reaction of Alizarin Red S with hydroxyapatite: stoichiometry and surface effect. Colloids Surf. 1992;66:181–7.
18. Wang D, Bradford SA, Harvey RW, Gao B, Cang L, Zhou D. Humic acid facilitates the transport of ARS-labeled hydroxyapatite nanoparticles in iron oxyhydroxide-coated sand. Environ Sci Technol. 2012;46:2738–45.
19. Liu H, Chen F, Xi P, Chen B, Huang L, Cheng J, et al. Biocompatible fluorescent hydroxyapatite: synthesis and live cell imaging applications. J Phys Chem C. 2011;115:18538–44.
20. Zhao X, Ng S, Heng BC, Guo J, Ma L, Tan TTY, et al. Cytotoxicity of hydroxyapatite nanoparticles is shape and cell dependent. Arch Toxicol. 2013;87:1037–52.

21. Hanson W. The photometric determination of phosphorus in fertilizers using the phosphovanado-molybdate complex. J Sci Food Agric. 1950;1:172–3.
22. Gouider M, Feki M, Sayadi S. Bioassay and use in irrigation of untreated and treated wastewaters from phosphate fertilizer industry. Ecotoxicol Environ Saf. 2010;73:932–8.
23. Chai C, Ben-Nissan B. Bioactive nanocrystalline sol–gel hydroxyapatite coatings. J Mater Sci Mater Med. 1999;10:465–9.
24. Xu Y, Wang D, Yang L, Tang H. Hydrothermal conversion of coral into hydroxyapatite. Mater Charact. 2001;47:83–7.
25. Klinkaewnarong J, Swatsitang E, Masingboon C, Seraphin S, Maensiri S. Synthesis and characterization of nanocrystalline HAp powders prepared by using aloe vera plant extracted solution. Curr Appl Phys. 2010;10:521–5.
26. Kumar R, Prakash K, Cheang P, Khor K. Temperature driven morphological changes of chemically precipitated hydroxyapatite nanoparticles. Langmuir. 2004;20:5196–200.
27. Wang G, Yang L, Jiang L, Shi M, Wei Z, Zhong W, et al. Simple combination of humic acid with biogenic hydroxyapatite achieved highly efficient removal of methylene blue from aqueous solution. RSC Adv. 2016;6:67888–97.
28. Ashok M, Sundaram NM, Kalkura SN. Crystallization of hydroxyapatite at physiological temperature. Mater Lett. 2003;57:2066–70.
29. Zhang C, Yang J, Quan Z, Yang P, Li C, Hou Z, et al. Hydroxyapatite nano- and microcrystals with multiform morphologies: controllable synthesis and luminescence properties. Cryst Growth Des. 2009;9:2725–33.
30. Li S, Bai H, Wang J, Jing X, Liu Q, Zhang M, et al. In situ grown of nano-hydroxyapatite on magnetic CaAl-layered double hydroxides and its application in uranium removal. Chem Eng J. 2012;193:372–80.
31. Gopi D, Nithiya S, Shinyjoy E, Kavitha L. Spectroscopic investigation on formation and growth of mineralized nanohydroxyapatite for bone tissue engineering applications. Spectrochim Acta Part A Mol Biomol Spectrosc. 2012;92:194–200.
32. Poinern G, Brundavanam R, Le XT, Djordjevic S, Prokic M, Fawcett D. Thermal and ultrasonic influence in the formation of nanometer scale hydroxyapatite bio-ceramic. Int J Nanomed. 2011;6:2083.
33. Pleshko N, Boskey A, Mendelsohn R. Novel infrared spectroscopic method for the determination of crystallinity of hydroxyapatite minerals. Biophys J. 1991;60:786–93.
34. Levinskas GJ, Neuman WF. The solubility of bone mineral. I. Solubility studies of synthetic hydroxylapatite. J Phys Chem. 1955;59:164–8.
35. Priyam A, Yadav N, Reddy PM, Afonso LO, Schultz AG, Singh PP. Fertilizing benefits of biogenic phosphorous nanonutrients on Solanum lycopersicum in soils with variable pH. Heliyon. 2022;8:09144.
36. Ye X, Wang G, Zhang Y, Zhao H. Hydroxyapatite nanoparticles in root cells: reducing the mobility and toxicity of Pb in rice. Environ Sci Nano. 2018;5:398–407.
37. Li Y, Fang F, Wei J, Wu X, Cui R, Li G, et al. Humic acid fertilizer improved soil properties and soil microbial diversity of continuous cropping peanut: a three-year experiment. Sci Rep. 2019;9:1–9.
38. Lv J, Christie P, Zhang S. Uptake, translocation, and transformation of metal-based nanoparticles in plants: recent advances and methodological challenges. Environ Sci Nano. 2019;6:41–59.
39. Bala N, Dey A, Das S, Basu R, Nandy P. Effect of hydroxyapatite nanorod on chickpea (Cicer arietinum) plant growth and its possible use as nano-fertilizer. Iranian Journal of Plant Physiology. 2014;4:1061–9.
40. Liu W, Wang S, Sun H, Zuo Q, Lai Y, Hou J. Impact of nanometer hydroxyapatite on seed germination and root border cell characteristics. RSC Adv. 2015;5:82726–31.
41. Dorozhkin SV, Epple M. Biological and medical significance of calcium phosphates. Angew Chem Int Ed. 2002;41:3130–46.
42. Dorozhkin SV. Calcium orthophosphates: occurrence, properties, biomineralization, pathological calcification and biomimetic applications. Biomatter. 2011;1:121–64.

Publisher's Note